

Period changes and four color light curves of the active overcontact binary V396 Monocerotis

Liu L.^{1,2,3,4}, Qian S.-B.^{1,2,3,4}, Liao W.-P.^{1,2,3,4}, He J.-J.^{1,2,3,4}, Zhu L.-Y.^{1,2,3,4}, Li L.-J.^{1,2,3,4}
and Zhao E.-G.^{1,2,3,4}

ABSTRACT

This paper analyzes the first secured four color light curves of V396 Mon using the 2003 version of the WD code. It is confirmed that V396 Mon is a shallow W-type contact binary system with a mass ratio $q = 2.554(\pm 0.004)$ and a degree of contact factor $f = 18.9\%(\pm 1.2\%)$. A period investigation based on all available data shows that the period of the system includes a long-term decrease ($dP/dt = -8.57 \times 10^{-8}$ days/year) and an oscillation ($A_3 = 0.^d0160$; $T_3 = 42.4$ years). They are caused by angular momentum loss (AML) and light-time effect, respectively. The suspect third body perhaps is a small M-type star (about 0.31 solar mass). Though some proofs show that this system has strong magnetic activity, through analyzing we found that the Applegate mechanism cannot explain the periodic changes. This binary is an especially important system according to Qian's statistics of contact binaries as its mass ratio lies near the proposed pivot point about which the physical structure of contact binaries supposedly oscillate.

Subject headings: Stars: binaries : close – Stars: binaries : eclipsing – Stars: individuals (V396 Mon) – Stars: evolution

1. Introduction

The light curves of V396 Monocerotis are continuous, sine-like. The primary minima are nearly of the same depth as the secondary minima. That is, V396 Mon has an EW-type

¹National Astronomical Observatories/Yunnan Observatory, Chinese Academy of Sciences, P.O. Box 110, 650011 Kunming, P.R. China (e-mail: creator_ll.student@sina.com; LiuL@ynao.ac.cn)

²Key Laboratory for the Structure and Evolution of Celestial Objects, Chinese Academy of Sciences, 650011 Kunming, P. R. China

³United Laboratory of Optical Astronomy, Chinese Academy of Sciences (ULOAC), 100012 Beijing, P. R. China

⁴Graduate School of the CAS, Beijing, P.R. China

light curve and was classified as a W Ursae Majoris eclipsing binary in the General Catalogue of Variable Stars (Kholopov 1985). A photographic light curve, times of light minimum, and ephemeris were given by Wachmann (1964). Subsequently, additional times of minima were published by Hoffmann (1983) and the Swiss Astronomical Society (BBSAG). Then, *BV* light curves observed in 1999, photoelectric solutions, and a period analysis were given by Yang & Liu (2001). Their conclusions were that V396 Mon is a W-type W UMa contact binary with a mass ratio of 0.402 and a cool spot presented on the secondary component which caused asymmetry of the light curves. One year later, Gu (2004) found the O’Connell effect (O’Connell 1951) in his observation to become very weak compared with that in Yang & Liu’s (2001) observation; he thought that this was an indication of starspot activity.

Generally, magnetic activity probably leads to an alternate period change of a close binary (e.g., Applegate 1992, Lanza et al. 1998). However, in Yang & Liu’s (2001) period analysis they did not find the expected variations owing to a lack of times of light minima data. Qian has published a series papers to discuss the long-term period variation of contact binary stars (i.e., Qian 2001a, b, 2003). His result is that this kind of variation may correlate with the mass of the primary component (M_1), and the mass ratio of the system (q). His statistic critical mass ratio q is 0.4. When $q > 0.4$, the secular period increases; contrary, $q < 0.4$, the secular period decreases. V396 Mon is important because of its mass ratio is around 0.4. As Qian said, such systems should be unstable and oscillate around the critical mass ratio. Therefore, V396 Mon becomes one of the monitoring targets in our contact binaries observation program running at Yunnan Observatory.

2. Observations

We carried out new CCD photometric observations of V396 Mon in *BVRI* bands on 2009 November 16 and 17, using the 1024×1024 PI1024 BFT camera attached to the 85-cm telescope at the Xinglong Station of National Astronomical Observatories of Chinese Academy of Sciences. The filter system was a standard Johnson-Cousins-Bessel multicolor CCD photometric system built on the primary focus (Zhou et al. 2009). The effective field of view is $16.'5 \times 16.'5$. The integration time for each image is 20 s. 2MASS06382732+0340193 and 2MASS06385506+0339462 were chosen as comparison and check star, respectively. These two stars are close to the target and their brightnesses are similar to the target. PHOT (measure magnitudes for a list of stars) of the aperture photometry package of IRAF was used to reduce the observed images, including a flat-fielding correction process. Through the observation we obtained *BVRI* light curves. The original data are listed in Tables 1 to 4. By calculating the phase of the observations with the equation $2455153.3614 + 0.^d39634359 \times E$,

the light curves are plotted in Figure 1. In this figure it is shown that the data of two days joined smooth and the light variation is typical of EW type. The magnitude difference between comparison star and check star is a constant, denoting the authenticity for the variations of the curves about V396 Mon. Since the light levels around the minima are symmetric, a quadratic polynomial fitting method was used to determine the times of minimum light by the least square method. In all, our new epochs of light minima were listed in Table 5.

The light curves in the V band obtained by Yang and Liu (2001) in 1999 and by the authors in 2009 are plotted in Figure 2. As shown in this figure, the light curves changed between 1999 January and 2009 November. The light curves observed in 2009 November are symmetric, while those obtained in 1999 January are asymmetric, which exhibit a typical O’Connell effect and show a much deeper primary minimum. The similar phenomenon was found out by Qian et al. (2006) when they analyzed a deep, low mass ratio overcontact binary system, AH Cancri. They did not interpret it then. Now, we are convinced that the changes of the light curves are caused by some cool star spots on the surface of the components. Actually, a cool star spot or several ones can make the primary minimum much deeper, which was proofed by Yang and Liu’s photometric solutions. Later, the spot disappeared, which was proofed by the photometric solutions of Gu (2004) and us. The present cool spots will alter the light curves very much, even strongly affecting the results of the photometric parameters.

3. Orbital period analysis

The first orbital period analysis of V396 Mon was given by Yang & Liu (2001). They collected 30 light minima and yield a corrected ephemeris,

$$\begin{aligned} \text{Min. I} &= 2451199.0715(\pm 0.0006) \\ &+ 0.^d3963410(\pm 0.0000007) \times E. \end{aligned} \quad (1)$$

As time passed, more and more minima of V396 Mon were obtained by various observers. We collected all available visual, photoelectric and CCD times of light minima, listing them in Table 6. We adopted the ephemeris $2455153.3614 + 0.^d39634498 \times E$ to modify its period, where 2455153.3614 is one of our times of light minima and 0.39634498 is found in GCVS (Samus et al. 2004). In calculation, the weight of visual data being set as 1 meanwhile that of the others being set as 8. A new corrected linear ephemeris was obtained:

$$\begin{aligned} \text{Min. I} &= 2455153.3766(\pm 0.0035) \\ &+ 0.^d39634359(\pm 0.00000010) \times E. \end{aligned} \quad (2)$$

The $(O - C)$ values with respect to the linear ephemeris are listed in the fifth column of Table 6. The corresponding $(O - C)_1$ diagram is displayed in Figure 3.

The general $(O - C)_1$ trend of V396 Mon shown in Figure 3 indicates the continuous period decrease. However a long-term period decrease alone (dashed line in Figure 3) cannot describe the $(O - C)_1$ curve very well; a period oscillation exists. Assuming that the period oscillation is cyclic, then, based on a least-square method, a sinusoidal term was added to a quadratic ephemeris to give a better fit to the $(O - C)_1$ curve (solid line in Figure 3). The result is

$$\begin{aligned}
 \text{Min. I} = & 2455153.3763(\pm 0.0053) \\
 & + 0.^d39634132(\pm 0.00000038) \times E \\
 & - 4.65(\pm 0.59) \times 10^{-11} \times E^2 \\
 & + 0.0160(\pm 0.0009) \sin[0.^{\circ}00921 \times E \\
 & - 65.^{\circ}5(\pm 12.^{\circ}2)].
 \end{aligned} \tag{3}$$

With the quadratic term in this equation, a secular period increase rate is determined, $dP/dt = -8.57 \times 10^{-8}$ days/year.

The $(O - C)_1$ values with respect to the quadratic ephemeris in Eq.(3) are shown in Figure 4. Although the visual data show large scatter, most of the photoelectric and CCD data lie close to the fitting line; an oscillation is presented in this figure. We have the relation,

$$\omega = 360^{\circ} P_e / T, \tag{4}$$

where P_e is the ephemeris period ($0.^d39634359$), the period of the orbital period oscillation is determined to be $T_3 = 42.4$ years.

4. Photometric solutions

V396 Mon is an ignored but important system. Yang and Liu (2001) determined its photometric solutions. They found the mass ratio q to be 0.402 and the fill-out factor f to be 5%, including a dark spot on the secondary component. But one year later, Gu (2004) found that the spot had dispersed. He derived a mass ratio of 2.937 (0.340).

To obtain initial input parameters, a q-search method with the 2003 version of the W-D program (Wilson & Devinney, 1971, Wilson, 1990, 1994, Wilson & Van Hamme, 2003) was used (Figure 5). We fixed q to 0.3, 0.4, 0.5 and so on, as figure 5 shows. It can be seen that

there are two lower points and the best value is around $q = 2.5$ (0.4), which is very close to the photometric value $q = 0.402$ (Yang & Liu 2001).

Throughout the solution the same value of temperature for star 1 (the star eclipsed at primary minimum) as that used by Yang & Liu (2001) ($T_1 = 6210\text{K}$) was chosen. The bolometric albedo $A_1 = A_2 = 0.5$ (Rucinski 1969) and the values of the gravity-darkening coefficient $g_1 = g_2 = 0.32$ (Lucy 1967) were used, which correspond to the common convective envelope of both components. Logarithm limb-darkening coefficients were used, taken from Claret & Gimenez (1990). We adjusted the mass ratio (q); the orbital inclination (i); the mean temperature of star 2 (T_2); the monochromatic luminosity of star 1 (L_1) and the dimensionless potential of star 1 ($\Omega_1 = \Omega_2$, mode 3 for contact configuration). Like Gu (2004)'s light curves, our multi-color light curves presented no O'Connell effect (O'Connell 1951). Period analysis indicated that the period oscillation may be caused by a light-time effect of a tertiary component, so we tried to adjusted the parameter l_3 in the W-D code. However, the numerical third light calculated by the program tended to negative. Therefore, in our final results we set third light equal to zero. The photometric solutions are listed in Table 7 and the theoretical light curves computed with those photometric elements are plotted in Figure 6. The geometrical structure of V396 Mon is displayed in Figure 7.

5. Discussions and conclusions

V396 Mon is a W-type marginal contact binary with a reliable photometric mass ratio 2.554 and a fill-factor 18.7%. The mass ratio $1/2.554 = 0.392$ is close to that of Yang and Liu (2001)'s result 0.402, but the fill-factors of the two results are significant difference ($18.7\% \pm 1.2\%$ and $4.7\% \pm 5.0\%$, respectively). The reasons are the system's period decease, the models simply unreliable in the sense of probable errors and the real much changes of the system in a decade. First, long-term period decrease cannot cause so big variations. The time scale of that is at least several million years, which is much longer than a decade. So it is impossible to see clear changes in systematic fashion in so short time. Second, although the models are simply, the prevenient practices tell us that the errors should not be so big. The third reason is the main one. The appearance of the cool spot strongly affects the results of the photometric parameters. More or less, two deferent light curves should have two deferent photometric solutions. Yang and Liu's (2001) light curves exist a star spot, which impacts on the solutions of the internal physical parameters. Moreover, the errors of their fill-factor is 5%, indicating the relative error is 106.3%, much bigger than 6.3% of ours. Thank to the disappeared cool spots, which make the light curves to restore their originally appearance. Hence, we think our results reveal the uncovered physical parameters and are

more reliable than Yang and Liu’s.

Although no spectroscopic elements have been published for this binary system, their absolute parameters can be estimated. Assuming that the primary components are normal, main sequence stars, we can estimate their masses as 0.36 and $0.92M_{\odot}$, corresponding to the results of W-D code. Combining with the photometric solutions and its period, we then estimated absolute parameters for the system ($R_1 = 0.84R_{\odot}$, $R_2 = 1.27R_{\odot}$; $L_1 = 0.947L_{\odot}$, $L_2 = 2.043L_{\odot}$). The evolutionary status of the components can be inferred from their mean densities (see for example, Mochnecki 1981, 1984). Using the following formulae (Kopal 1959),

$$\overline{\rho}_1 = \frac{0.079}{V_1(1+q)P^2}, \quad \overline{\rho}_2 = \frac{0.079q}{V_2(1+q)P^2}, \quad (5)$$

where $V_{1,2}$ are the volumes of the components using the separation A as the unit of length, we determined the mean densities (ρ_1, ρ_2) of the two components to be $1.112 \rho_{\odot}$ and $0.809 \rho_{\odot}$. The corresponding logarithms of the mean densities are 0.046 and -0.092 , which are lower than those of zero-age main sequence (ZAMS) stars of the same spectral type, especially for the less massive components. This indicates that the components in both systems have already moved away from the ZAMS line to a greater or lesser extent.

The period variation of V396 Mon represented is very complex. Based on all available photoelectric and CCD eclipse times, the period changes of the contact binary star were discussed in the previous section. First, the orbital period was revised as 0.39634359 days by using the 118 visual, CCD and photoelectric timings being listed in Table 6. Second, the general ($O - C$) trend reveals a long-term period decrease at a rate of $dP/dt = -8.57 \times 10^{-8}$ days/year. In addition, a period oscillation ($A_3 \sim 0^d.0160$) was discovered superimposed on the period decrease. If this period decrease is due to a conservative mass transfer from the more massive component to the less massive one, then with the absolute parameters derived by the present paper and by using the well-known equation,

$$\frac{\dot{P}}{P} = 3 \frac{\dot{M}_2}{M_2} \left(\frac{M_2}{M_1} - 1 \right), \quad (6)$$

the mass transfer rate is estimated to be, $dM_2/dt = -4.26 \times 10^{-8} M_{\odot}/year$. The negative sign implies that the more massive component M_2 is losing its mass. The timescale of mass transfer is $\tau \sim M_2/\dot{M}_2 \sim 2.2 \times 10^7$ years which is 4 times the thermal time scale of the more massive component. However, having considered the strong magnetic activity of the system (Gu 2004 and our discussions above), the long-term period decrease can be reasonably explained as the results of an enhanced stellar wind and angular momentum loss (AML). Table 8 lists some contact binary systems that exhibit long-term period decreases.

We now address the short-term period oscillation with $T_3 = 42.4$ years, $A_3 = 0.0160$

days. There are two main ways to interpret these observations: the Applegate mechanism and light-time effect.

The Applegate mechanism says that the cyclic period change is caused by magnetic activity-driven variations in the quadrupole moment of the solar-type components (e.g., Applegate 1992, Lanza et al. 1998). According to the formula (Lanza & Rodonò 2002; Rovithis-Livaniou et al. 2000),

$$\frac{\Delta P}{P} = -9 \frac{\Delta Q}{Ma^2}, \quad (7)$$

$$\Delta P = \sqrt{[1 - \cos(2\pi P/P_3)]} \times A_3, \quad (8)$$

we got the needed quadrupole moment were $\Delta Q_1 = 1.41 \times 10^{49}$ and $\Delta Q_2 = 3.61 \times 10^{49} g \cdot cm^2$. However, for active close binary stars, the typical values range from 10^{51} to $10^{52} g \cdot cm^2$. Therefore the Applegate mechanism probably does not describe the short-term period changes in V396 Mon.

The most likely explanation of the period oscillation is that a light-time effect of a tertiary component causes this phenomenon. By using this equation:

$$f(m) = \frac{4\pi^2}{GT_3^2} \times (a'_{12} \sin i')^3, \quad (9)$$

where $a'_{12} \sin i' = A_3 \times c$ (where c is the speed of light), the mass function from the tertiary component can be computed with the following equation:

$$f(m) = \frac{(M_3 \sin i')^3}{(M_1 + M_2 + M_3)^2}. \quad (10)$$

Assuming the third body and the central system are coplanar, and taking the estimated physical parameters given in the first paragraph of this section, the mass and the orbital radius of the suspect third companion can be estimated. The smallest mass of a tertiary companion should be $m_3 = 0.31M_\odot$ with a separation of 14.2 AU. The luminosity of such a small M main sequence star is only $0.026L_\odot$, 0.87% of the whole system. This could explain why we did not find third light in W-D solutions.

In summary, V396 Mon is a middle mass ratio shallow contact binary. Although previous light curves showed evidence of spot activity, our current observations seem to indicate a lack of any light curve asymmetries. The periodic variation of its period changes is most likely caused by a third body, probably a small M star. To more accurately determine the absolute parameters of V396 Mon, a precision radial velocity curve must be secured. If we can determine that its true mass ratio is indeed close to 0.4 (the 0.4 mass ratio argument of Qian), this binary system becomes an especially important system and is worth to do a deep research in the future.

This work is partly supported by Yunnan Natural Science Foundation (2008CD157), Chinese Natural Science Foundation (No.10973037 and No.10903026), The Ministry of Science and Technology of the Peoples Republic of China through grant 2007CB815406 and The Chinese Academy of Sciences grant No. O8ZKY11001. New observations of the system were obtained with the 1-m telescope at Yunnan Observatory and 85-cm telescope at Xinglong observation base.

We are especially indebted to the anonymous referee who given us useful comments and cordial suggestions, which helped us to improve the paper greatly.

REFERENCES

- Applegate, J. H., 1992 ApJ, 385, 621
- Claret, A. and Gimenez, A., 1990, A&A, 230, 412
- Gu, S. H. 2004, AN, 325, 661
- Kholopov, P. N. et al., 1985, General Catalogue of Variable Stars, Vol. 2 (4th ed. ; Moscow: Nauka), 190
- Kopal, Z. 1959, Close Binary Systems, Chapman & Hall, London
- Lanza, A. F., Rodonò, M., 2002, AN, 323, 424
- Lanza, A. F., Rodonò, M. and Rosner, R., 1998, MNRAS, 296, 893
- Lucy, L. B., 1967, Zeitschrift für Astrophysik, 65, 89
- Mochnecki, S. W., 1981, ApJ, 245, 650
- Mochnecki, S. W., 1984, ApJS, 55, 551
- O’Connell, D. J. K. 1951, MNRAS, 111, 642O
- Qian, S.-B., 2001a, MNRAS, 328, 635
- Qian, S.-B., 2001b, MNRAS, 328, 914
- Qian, S.-B., 2003, MNRAS, 342, 1260
- Qian, S.-B., Liu, L., Soonthornthum, B., Zhu, L.-Y., He, J.-J., 2006, AJ, 131, 3028
- Rovithis-Livaniou H., Kranidiotis A. N., Rovithis P. & Athanassiades G., 2000 A&A, 354, 904
- Rucinski, S. M., 1969, A&A, 19, 245
- Samus, N. N. et al., 2004, Combined General Catalog of Variable Stars, GCVS4.2, 2004 Ed.

- Tout, C. A., Hall, D. S., 1991, MNRAS, 253, 9T
- Tout, C. A., Eggleton, P. P., 1988, MNRAS, 231, 823T
- Wachmann, A. A. 1964, Astron. Abh. Hamburger Sternw., 7, 155
- Wilson, R. E., 1990, ApJ, 356, 613
- Wilson, R. E., 1994, PASP, 106, 921
- Wilson, R. E., & Devinney, E. J., 1971, ApJ, 166, 605
- Wilson, R. E. & Van Hamme, W. 2003, Computing Binary Stars Observables, the 4th edition of the W-D programe.
- Yang, Y. L. & Liu, Q. Y., 2001, AJ, 122, 425
- Zhou, Ai-Ying, Jiang, Xiao-Jun, Zhang, Yan-Ping, Wei, Jian-Yan, 2009, RAA, 9, 349Z

Table 1: The original data of V396 Mon in B band observed by 85cm telescope at Xinglong base, National Observatory. Hel. JD 2455100+

Hel.JD	Δm	Hel.JD	Δm	Hel.JD	Δm	Hel.JD	Δm	Hel.JD	Δm	Hel.JD	Δm	Hel.JD	Δm
52.2027	-.064	52.2633	-.404	52.3239	-.256	52.3845	.176	53.2474	-.392	53.3079	-.278	53.3684	.222
52.2042	-.096	52.2648	-.403	52.3254	-.234	52.3860	.141	53.2488	-.398	53.3093	-.272	53.3699	.214
52.2056	-.096	52.2662	-.411	52.3268	-.222	52.3874	.125	53.2502	-.390	53.3108	-.281	53.3713	.223
52.2071	-.120	52.2677	-.416	52.3283	-.223	52.3889	.095	53.2517	-.408	53.3122	-.268	53.3727	.224
52.2085	-.143	52.2691	-.406	52.3297	-.211	52.3903	.075	53.2531	-.392	53.3136	-.257	53.3742	.208
52.2100	-.167	52.2705	-.418	52.3311	-.197	52.3917	.036	53.2546	-.404	53.3151	-.238	53.3756	.186
52.2114	-.171	52.2720	-.393	52.3326	-.178	52.3932	.034	53.2560	-.389	53.3165	-.216	53.3771	.158
52.2128	-.184	52.2734	-.416	52.3340	-.165	52.3946	.018	53.2574	-.406	53.3180	-.213	53.3785	.139
52.2143	-.200	52.2749	-.416	52.3355	-.130	52.3961	-.005	53.2589	-.404	53.3194	-.208	53.3799	.104
52.2157	-.208	52.2763	-.408	52.3369	-.134	52.3975	-.030	53.2603	-.403	53.3208	-.198	53.3814	.101
52.2172	-.226	52.2778	-.411	52.3384	-.109	52.3990	-.041	53.2618	-.398	53.3223	-.178	53.3828	.073
52.2186	-.252	52.2792	-.409	52.3398	-.087	52.4004	-.070	53.2632	-.409	53.3237	-.164	53.3843	.046
52.2201	-.225	52.2807	-.401	52.3413	-.091	52.4018	-.084	53.2647	-.400	53.3252	-.146	53.3857	.018
52.2215	-.268	52.2821	-.405	52.3427	-.054	52.4033	-.104	53.2661	-.400	53.3266	-.137	53.3871	.014
52.2229	-.261	52.2835	-.401	52.3441	-.032	52.4047	-.125	53.2675	-.396	53.3280	-.112	53.3886	-.023
52.2244	-.273	52.2850	-.416	52.3456	-.004	52.4062	-.140	53.2690	-.397	53.3295	-.089	53.3900	-.039
52.2258	-.291	52.2864	-.407	52.3470	.004	52.4076	-.147	53.2704	-.400	53.3309	-.076	53.3915	-.056
52.2273	-.294	52.2879	-.397	52.3485	.024	52.4091	-.174	53.2719	-.399	53.3324	-.053	53.3929	-.095
52.2287	-.291	52.2893	-.398	52.3499	.059	52.4105	-.177	53.2733	-.400	53.3338	-.032	53.3944	-.098
52.2302	-.303	52.2907	-.403	52.3513	.081	52.4119	-.194	53.2747	-.392	53.3352	-.004	53.3958	-.127
52.2316	-.309	52.2922	-.394	52.3528	.110	52.4134	-.204	53.2762	-.393	53.3367	.007	53.3972	-.127
52.2330	-.312	52.2936	-.386	52.3542	.136	52.4148	-.195	53.2776	-.383	53.3381	.018	53.3987	-.137
52.2345	-.320	52.2951	-.387	52.3557	.165	52.4163	-.229	53.2791	-.387	53.3396	.064	53.4001	-.173
52.2359	-.328	52.2965	-.371	52.3571	.179	52.4177	-.230	53.2805	-.380	53.3410	.089	53.4016	-.187
52.2374	-.332	52.2980	-.372	52.3586	.192	52.4192	-.255	53.2819	-.387	53.3425	.119	53.4030	-.190
52.2388	-.333	52.2994	-.364	52.3600	.222	52.4206	-.281	53.2834	-.371	53.3439	.147	53.4044	-.208
52.2403	-.335	52.3008	-.369	52.3614	.221	52.4235	-.292	53.2848	-.377	53.3453	.155	53.4059	-.220
52.2417	-.357	52.3023	-.376	52.3629	.237	53.2257	-.323	53.2863	-.369	53.3468	.165	53.4073	-.254
52.2431	-.356	52.3037	-.359	52.3643	.230	53.2272	-.320	53.2877	-.366	53.3482	.181	53.4088	-.248
52.2446	-.361	52.3052	-.360	52.3658	.251	53.2286	-.333	53.2891	-.363	53.3497	.202	53.4102	-.259
52.2460	-.363	52.3066	-.343	52.3672	.245	53.2301	-.339	53.2906	-.348	53.3511	.219	53.4117	-.240
52.2475	-.367	52.3081	-.336	52.3687	.254	53.2315	-.346	53.2920	-.340	53.3525	.208	53.4131	-.238
52.2489	-.368	52.3095	-.325	52.3701	.260	53.2329	-.352	53.2935	-.351	53.3540	.207	53.4145	-.270
52.2503	-.381	52.3110	-.333	52.3715	.238	53.2344	-.344	53.2949	-.338	53.3554	.222	53.4160	-.277
52.2518	-.385	52.3124	-.320	52.3730	.243	53.2358	-.365	53.2963	-.332	53.3569	.210	53.4174	-.276
52.2532	-.385	52.3138	-.318	52.3744	.239	53.2373	-.361	53.2978	-.323	53.3583	.233	53.4189	-.297
52.2547	-.389	52.3153	-.308	52.3759	.247	53.2387	-.363	53.2992	-.332	53.3598	.221	53.4203	-.294
52.2561	-.396	52.3167	-.295	52.3773	.244	53.2401	-.382	53.3007	-.314	53.3612	.211		
52.2576	-.392	52.3182	-.289	52.3788	.229	53.2416	-.372	53.3021	-.314	53.3626	.227		
52.2590	-.392	52.3196	-.284	52.3802	.228	53.2430	-.381	53.3036	-.308	53.3641	.231		
52.2605	-.399	52.3210	-.277	52.3816	.222	53.2445	-.379	53.3050	-.285	53.3655	.216		
52.2619	-.397	52.3225	-.261	52.3831	.194	53.2459	-.385	53.3064	-.301	53.3670	.230		

Table 2: The original data of V396 Mon in V band observed by 85cm telescope at Xinglong base, National Observatory. Hel. JD 2455100+

Hel.JD	Δm	Hel.JD	Δm	Hel.JD	Δm	Hel.JD	Δm	Hel.JD	Δm	Hel.JD	Δm	Hel.JD	Δm
52.2031	.102	52.2637	-.224	52.3243	-.070	52.3849	.319	53.2449	-.194	53.3054	-.108	53.3659	.374
52.2046	.083	52.2652	-.221	52.3258	-.058	52.3864	.306	53.2463	-.199	53.3068	-.105	53.3674	.376
52.2060	.060	52.2666	-.210	52.3272	-.046	52.3878	.284	53.2478	-.197	53.3083	-.100	53.3688	.390
52.2075	.050	52.2681	-.212	52.3287	-.026	52.3893	.263	53.2492	-.199	53.3097	-.095	53.3703	.375
52.2089	.027	52.2695	-.221	52.3301	-.028	52.3907	.235	53.2506	-.204	53.3112	-.083	53.3717	.376
52.2104	.008	52.2709	-.228	52.3315	-.011	52.3921	.199	53.2521	-.200	53.3126	-.081	53.3731	.370
52.2118	.001	52.2724	-.224	52.3330	.000	52.3936	.191	53.2535	-.208	53.3140	-.067	53.3746	.360
52.2132	-.009	52.2738	-.218	52.3344	.007	52.3950	.171	53.2549	-.208	53.3155	-.062	53.3760	.341
52.2147	-.024	52.2753	-.226	52.3359	.035	52.3965	.145	53.2564	-.207	53.3169	-.040	53.3775	.317
52.2161	-.050	52.2767	-.228	52.3373	.049	52.3979	.125	53.2578	-.198	53.3184	-.032	53.3789	.294
52.2176	-.050	52.2782	-.234	52.3388	.069	52.3993	.110	53.2593	-.217	53.3198	-.028	53.3803	.288
52.2190	-.065	52.2796	-.226	52.3402	.088	52.4008	.092	53.2607	-.206	53.3212	-.025	53.3818	.252
52.2204	-.083	52.2810	-.213	52.3417	.097	52.4022	.080	53.2622	-.204	53.3227	.003	53.3832	.230
52.2219	-.082	52.2825	-.219	52.3431	.119	52.4037	.069	53.2636	-.218	53.3241	.024	53.3847	.209
52.2233	-.081	52.2839	-.213	52.3445	.142	52.4051	.047	53.2651	-.208	53.3256	.033	53.3861	.176
52.2248	-.101	52.2854	-.214	52.3460	.159	52.4066	.038	53.2665	-.218	53.3270	.052	53.3875	.167
52.2262	-.090	52.2868	-.222	52.3474	.183	52.4080	.013	53.2679	-.220	53.3284	.065	53.3890	.136
52.2277	-.104	52.2883	-.215	52.3489	.220	52.4095	.016	53.2694	-.212	53.3299	.088	53.3904	.128
52.2291	-.121	52.2897	-.218	52.3503	.236	52.4109	.007	53.2708	-.203	53.3313	.116	53.3919	.097
52.2306	-.119	52.2911	-.199	52.3517	.257	52.4123	-.014	53.2723	-.211	53.3328	.140	53.3933	.072
52.2320	-.141	52.2926	-.194	52.3532	.286	52.4138	-.007	53.2737	-.206	53.3342	.153	53.3948	.058
52.2334	-.137	52.2940	-.199	52.3546	.293	52.4152	-.035	53.2751	-.208	53.3356	.176	53.3962	.051
52.2349	-.133	52.2955	-.192	52.3561	.335	52.4167	-.037	53.2766	-.198	53.3371	.189	53.3976	.025
52.2363	-.139	52.2969	-.196	52.3575	.340	52.4181	-.065	53.2780	-.191	53.3385	.230	53.3991	.007
52.2378	-.141	52.2984	-.191	52.3590	.363	52.4196	-.067	53.2795	-.207	53.3400	.246	53.4005	.003
52.2392	-.164	52.2998	-.187	52.3604	.389	52.4210	-.101	53.2809	-.191	53.3414	.256	53.4020	.001
52.2406	-.165	52.3012	-.170	52.3618	.387	52.4224	-.075	53.2823	-.193	53.3429	.276	53.4034	-.009
52.2421	-.163	52.3027	-.176	52.3633	.404	52.4239	-.099	53.2838	-.188	53.3443	.307	53.4048	-.028
52.2435	-.164	52.3041	-.167	52.3647	.391	52.4253	-.066	53.2852	-.184	53.3457	.336	53.4063	-.043
52.2450	-.171	52.3056	-.152	52.3662	.395	53.2261	-.132	53.2867	-.179	53.3472	.354	53.4077	-.054
52.2464	-.188	52.3070	-.155	52.3676	.403	53.2276	-.138	53.2881	-.170	53.3486	.362	53.4092	-.067
52.2479	-.189	52.3085	-.143	52.3691	.410	53.2290	-.135	53.2895	-.170	53.3501	.374	53.4106	-.082
52.2493	-.183	52.3099	-.133	52.3705	.404	53.2305	-.158	53.2910	-.170	53.3515	.366	53.4120	-.085
52.2507	-.193	52.3113	-.126	52.3719	.411	53.2319	-.153	53.2924	-.171	53.3529	.369	53.4135	-.097
52.2522	-.197	52.3128	-.132	52.3734	.401	53.2333	-.163	53.2938	-.158	53.3544	.375	53.4149	-.092
52.2536	-.196	52.3142	-.126	52.3748	.402	53.2348	-.173	53.2953	-.152	53.3558	.379	53.4164	-.109
52.2551	-.189	52.3157	-.118	52.3763	.399	53.2362	-.165	53.2967	-.151	53.3573	.371	53.4178	-.120
52.2565	-.205	52.3171	-.098	52.3777	.395	53.2377	-.179	53.2982	-.141	53.3587	.382	53.4193	-.131
52.2580	-.212	52.3186	-.101	52.3792	.391	53.2391	-.174	53.2996	-.130	53.3601	.380	53.4207	-.119
52.2594	-.209	52.3200	-.096	52.3806	.386	53.2405	-.189	53.3011	-.136	53.3616	.389		
52.2609	-.224	52.3214	-.088	52.3820	.364	53.2420	-.178	53.3025	-.115	53.3630	.402		
52.2623	-.216	52.3229	-.080	52.3835	.341	53.2434	-.194	53.3039	-.122	53.3645	.382		

Table 3: The original data of V396 Mon in R band observed by 85cm telescope at Xinglong base, National Observatory. Hel. JD 2455100+

Hel.JD	Δm	Hel.JD	Δm	Hel.JD	Δm	Hel.JD	Δm	Hel.JD	Δm	Hel.JD	Δm	Hel.JD	Δm
52.2035	.185	52.2655	-.128	52.3261	.040	52.3867	.385	53.2466	-.111	53.3072	-.012	53.3677	.465
52.2049	.152	52.2670	-.129	52.3276	.065	52.3882	.358	53.2481	-.101	53.3086	-.012	53.3691	.474
52.2064	.147	52.2684	-.127	52.3290	.060	52.3896	.344	53.2495	-.098	53.3100	-.002	53.3706	.444
52.2078	.127	52.2698	-.123	52.3304	.084	52.3910	.317	53.2510	-.115	53.3115	.012	53.3720	.463
52.2093	.114	52.2713	-.124	52.3319	.101	52.3925	.286	53.2524	-.120	53.3129	.017	53.3735	.452
52.2107	.098	52.2727	-.116	52.3333	.094	52.3939	.285	53.2539	-.107	53.3144	.031	53.3749	.445
52.2121	.077	52.2742	-.122	52.3348	.112	52.3954	.256	53.2553	-.104	53.3158	.037	53.3764	.402
52.2136	.079	52.2756	-.124	52.3362	.139	52.3968	.242	53.2567	-.130	53.3173	.046	53.3778	.392
52.2150	.071	52.2771	-.129	52.3377	.162	52.3983	.215	53.2582	-.110	53.3187	.050	53.3792	.378
52.2165	.058	52.2785	-.119	52.3391	.163	52.3997	.203	53.2596	-.107	53.3201	.069	53.3807	.355
52.2179	.042	52.2799	-.119	52.3405	.183	52.4011	.183	53.2611	-.117	53.3216	.087	53.3821	.344
52.2194	.028	52.2814	-.120	52.3420	.201	52.4026	.166	53.2625	-.115	53.3230	.100	53.3836	.312
52.2222	.020	52.2828	-.115	52.3434	.223	52.4040	.151	53.2639	-.117	53.3245	.111	53.3850	.289
52.2237	.004	52.2843	-.110	52.3449	.267	52.4055	.135	53.2654	-.116	53.3259	.141	53.3864	.269
52.2251	-.009	52.2857	-.115	52.3463	.259	52.4069	.120	53.2668	-.121	53.3273	.141	53.3879	.242
52.2266	-.008	52.2872	-.106	52.3478	.285	52.4083	.112	53.2683	-.104	53.3288	.175	53.3893	.218
52.2280	-.008	52.2886	-.103	52.3492	.308	52.4098	.091	53.2697	-.093	53.3302	.172	53.3908	.221
52.2294	-.023	52.2900	-.102	52.3506	.328	52.4112	.084	53.2711	-.104	53.3317	.195	53.3922	.192
52.2309	-.024	52.2915	-.107	52.3521	.354	52.4127	.063	53.2726	-.116	53.3331	.217	53.3936	.167
52.2323	-.021	52.2929	-.104	52.3535	.385	52.4141	.056	53.2740	-.111	53.3346	.238	53.3951	.158
52.2338	-.041	52.2944	-.094	52.3550	.398	52.4156	.048	53.2755	-.099	53.3360	.256	53.3965	.128
52.2352	-.060	52.2958	-.101	52.3564	.418	52.4170	.046	53.2769	-.105	53.3374	.286	53.3980	.115
52.2367	-.038	52.2973	-.095	52.3579	.459	52.4185	.020	53.2783	-.099	53.3389	.298	53.3994	.104
52.2381	-.041	52.2987	-.098	52.3593	.460	52.4199	.016	53.2798	-.097	53.3403	.325	53.4009	.107
52.2396	-.058	52.3001	-.074	52.3607	.451	52.4213	.013	53.2812	-.103	53.3417	.367	53.4023	.074
52.2410	-.055	52.3016	-.077	52.3622	.474	52.4228	.001	53.2827	-.091	53.3432	.371	53.4037	.071
52.2424	-.070	52.3030	-.077	52.3636	.480	52.4242	-.012	53.2841	-.083	53.3446	.394	53.4052	.045
52.2439	-.072	52.3045	-.060	52.3651	.471	52.4257	-.010	53.2855	-.089	53.3461	.417	53.4066	.054
52.2453	-.067	52.3059	-.065	52.3665	.485	53.2265	-.041	53.2870	-.080	53.3475	.444	53.4081	.036
52.2468	-.078	52.3074	-.064	52.3680	.481	53.2279	-.045	53.2884	-.076	53.3490	.439	53.4095	.037
52.2482	-.092	52.3088	-.051	52.3694	.481	53.2294	-.051	53.2899	-.078	53.3504	.458	53.4110	.007
52.2496	-.100	52.3102	-.033	52.3708	.484	53.2308	-.059	53.2913	-.073	53.3518	.467	53.4124	.025
52.2511	-.100	52.3117	-.054	52.3723	.482	53.2322	-.053	53.2928	-.063	53.3533	.460	53.4138	.007
52.2525	-.097	52.3131	-.033	52.3737	.493	53.2337	-.071	53.2942	-.056	53.3547	.477	53.4153	.009
52.2540	-.095	52.3146	-.023	52.3752	.501	53.2351	-.070	53.2956	-.054	53.3562	.470	53.4167	-.025
52.2554	-.098	52.3160	-.010	52.3766	.486	53.2366	-.066	53.2971	-.054	53.3576	.467	53.4182	-.025
52.2569	-.102	52.3175	-.016	52.3781	.479	53.2380	-.078	53.2985	-.049	53.3591	.454	53.4196	-.022
52.2583	-.126	52.3189	.005	52.3795	.477	53.2394	-.084	53.3000	-.032	53.3605	.467	53.4210	-.027
52.2597	-.107	52.3203	.008	52.3809	.463	53.2409	-.096	53.3014	-.037	53.3619	.450		
52.2612	-.108	52.3218	.014	52.3824	.450	53.2423	-.092	53.3028	-.031	53.3634	.451		
52.2626	-.110	52.3232	.019	52.3838	.424	53.2438	-.090	53.3043	-.028	53.3648	.470		
52.2641	-.125	52.3247	.036	52.3853	.396	53.2452	-.095	53.3057	-.013	53.3663	.452		

Table 4: The original data of V396 Mon in I band observed by 85cm telescope at Xinglong base, National Observatory. Hel. JD 2455100+

Hel.JD	Δm	Hel.JD	Δm	Hel.JD	Δm	Hel.JD	Δm	Hel.JD	Δm	Hel.JD	Δm	Hel.JD	Δm
52.2038	.284	52.2644	-.008	52.3250	.146	52.3856	.494	53.2455	.011	53.3075	.095	53.3680	.555
52.2052	.266	52.2658	-.008	52.3264	.155	52.3870	.490	53.2470	.011	53.3089	.102	53.3695	.559
52.2067	.255	52.2673	-.010	52.3279	.171	52.3885	.466	53.2498	-.002	53.3104	.113	53.3709	.550
52.2081	.224	52.2687	.000	52.3293	.177	52.3899	.429	53.2513	-.014	53.3118	.112	53.3723	.550
52.2096	.224	52.2702	-.007	52.3308	.183	52.3913	.422	53.2527	-.007	53.3132	.127	53.3738	.546
52.2110	.198	52.2716	-.015	52.3322	.211	52.3928	.392	53.2542	-.002	53.3147	.135	53.3752	.515
52.2124	.179	52.2730	-.008	52.3336	.213	52.3942	.385	53.2556	.005	53.3161	.144	53.3767	.500
52.2139	.166	52.2745	-.002	52.3351	.231	52.3957	.362	53.2571	-.007	53.3176	.148	53.3781	.494
52.2153	.158	52.2759	-.013	52.3365	.240	52.3971	.334	53.2585	-.009	53.3190	.178	53.3796	.459
52.2168	.142	52.2774	-.015	52.3380	.267	52.3986	.332	53.2599	-.015	53.3204	.175	53.3810	.432
52.2182	.149	52.2788	-.011	52.3394	.272	52.4000	.310	53.2614	-.010	53.3219	.193	53.3824	.428
52.2197	.142	52.2803	-.017	52.3409	.302	52.4014	.292	53.2628	-.019	53.3233	.197	53.3839	.399
52.2211	.125	52.2817	-.008	52.3423	.308	52.4029	.261	53.2643	-.014	53.3248	.223	53.3853	.379
52.2225	.126	52.2831	-.013	52.3437	.339	52.4043	.258	53.2657	-.014	53.3262	.230	53.3867	.343
52.2240	.115	52.2846	-.013	52.3452	.351	52.4058	.221	53.2671	-.009	53.3277	.236	53.3882	.342
52.2254	.109	52.2860	-.011	52.3466	.359	52.4072	.224	53.2686	-.008	53.3291	.274	53.3896	.320
52.2269	.105	52.2875	-.006	52.3481	.386	52.4087	.232	53.2700	-.010	53.3305	.290	53.3911	.282
52.2283	.086	52.2889	.010	52.3495	.417	52.4101	.196	53.2715	.004	53.3320	.302	53.3925	.282
52.2298	.087	52.2903	.007	52.3510	.444	52.4115	.194	53.2729	-.006	53.3334	.317	53.3940	.259
52.2312	.093	52.2918	.006	52.3524	.468	52.4130	.176	53.2743	-.001	53.3349	.334	53.3954	.243
52.2326	.068	52.2932	.008	52.3538	.470	52.4144	.170	53.2758	.000	53.3363	.369	53.3968	.221
52.2341	.072	52.2947	.012	52.3553	.499	52.4159	.161	53.2772	.000	53.3377	.377	53.3983	.221
52.2355	.079	52.2961	.005	52.3567	.511	52.4173	.145	53.2787	-.005	53.3392	.410	53.3997	.198
52.2370	.060	52.2976	.012	52.3582	.532	52.4188	.123	53.2801	.010	53.3406	.419	53.4012	.183
52.2384	.046	52.2990	.030	52.3596	.578	52.4202	.124	53.2815	.017	53.3421	.445	53.4026	.168
52.2399	.050	52.3005	.039	52.3611	.552	52.4216	.113	53.2830	.030	53.3435	.463	53.4041	.154
52.2413	.050	52.3019	.032	52.3625	.542	52.4231	.123	53.2844	.021	53.3449	.491	53.4055	.146
52.2427	.036	52.3033	.033	52.3639	.585	52.4245	.091	53.2859	.028	53.3464	.504	53.4069	.139
52.2442	.046	52.3048	.045	52.3654	.550	52.4260	.073	53.2873	.023	53.3478	.523	53.4084	.139
52.2456	.025	52.3062	.050	52.3668	.580	53.2268	.064	53.2887	.020	53.3493	.544	53.4098	.124
52.2471	.018	52.3077	.052	52.3683	.561	53.2282	.052	53.2902	.035	53.3507	.541	53.4113	.120
52.2485	.029	52.3091	.069	52.3697	.576	53.2297	.052	53.2916	.034	53.3522	.557	53.4127	.121
52.2500	.024	52.3105	.068	52.3711	.581	53.2311	.056	53.2931	.029	53.3536	.550	53.4141	.108
52.2514	.010	52.3120	.067	52.3726	.573	53.2325	.039	53.2945	.054	53.3550	.553	53.4156	.110
52.2528	.013	52.3134	.074	52.3740	.568	53.2340	.042	53.2959	.049	53.3565	.554	53.4170	.086
52.2543	.003	52.3149	.075	52.3755	.572	53.2354	.035	53.2974	.061	53.3579	.549	53.4185	.086
52.2557	.012	52.3163	.100	52.3769	.582	53.2369	.035	53.2988	.056	53.3594	.568	53.4199	.055
52.2572	.011	52.3178	.095	52.3784	.565	53.2383	.017	53.3003	.058	53.3608	.547	53.4214	.053
52.2586	.003	52.3192	.099	52.3798	.561	53.2397	.024	53.3017	.064	53.3622	.558	53.4228	.065
52.2601	.003	52.3207	.113	52.3813	.560	53.2412	.025	53.3031	.061	53.3637	.546		
52.2615	.002	52.3221	.125	52.3827	.541	53.2426	.012	53.3046	.061	53.3651	.578		
52.2629	.000	52.3235	.137	52.3841	.524	53.2441	.009	53.3060	.088	53.3666	.567		

Table 5: New CCD times of light minima for V396 Mon.

JD (Hel.)	Error (days)	Method	Min.	Filters	Telescope
2452705.1581	± 0.0005	CCD	I	V	1m
2452944.3501	± 0.0011	CCD	II	V	1m
2452944.3524	± 0.0003	CCD	II	B	1m
2452945.3409	± 0.0006	CCD	I	V	1m
2452945.3394	± 0.0008	CCD	I	B	1m
2454917.14503	± 0.00170	CCD	II	I	1m
2455152.37049	± 0.00015	CCD	II	B	85cm
2455152.37072	± 0.00020	CCD	II	V	85cm
2455152.37035	± 0.00016	CCD	II	R	85cm
2455152.37052	± 0.00014	CCD	II	I	85cm
2455153.36162	± 0.00018	CCD	I	B	85cm
2455153.36139	± 0.00016	CCD	I	V	85cm
2455153.36151	± 0.00018	CCD	I	R	85cm
2455153.36122	± 0.00017	CCD	I	I	85cm

1m denotes the 1 meter R-C reflect telescope in Yunnan Observatory. 85cm denotes the 85 cm reflect telescope in Xinglong Observation base.

Table 6. Times of light minima of V396 MON.

Hel.JD	Type	Method	E	$(O - C)_1$	$(O - C)_2$	Reference
29691.435	p	pg	-64242	-0.03690	0.00937	Wachmann 1964
29696.395	s	pg	-64229.5	-0.03119	0.01503	Wachmann 1964
30021.405	s	pg	-63409.5	-0.02293	0.02028	Wachmann 1964
30024.360	p	pg	-63402	-0.04051	0.00268	Wachmann 1964
30025.360	s	pg	-63399.5	-0.03137	0.01181	Wachmann 1964
30026.350	p	pg	-63397	-0.03223	0.01094	Wachmann 1964
30069.375	s	pg	-63288.5	-0.01051	0.03227	Wachmann 1964
30072.335	p	pg	-63281	-0.02308	0.01966	Wachmann 1964
30373.340	s	pg	-62521.5	-0.04104	-0.00100	Wachmann 1964
31142.445	p	pg	-60581	-0.04077	-0.00743	Wachmann 1964
31144.496	p	pg	-60576	0.02852	0.06183	Wachmann 1964
31803.575	p	pg	-58913	-0.01187	0.01598	Wachmann 1964
31845.415	s	pg	-58807.5	0.01388	0.04139	Wachmann 1964
32233.410	s	pg	-57828.5	-0.01149	0.01293	Wachmann 1964
33220.515	p	pg	-55338	-0.00019	0.01678	Wachmann 1964
33294.425	s	pg	-55151.5	-0.00827	0.00817	Wachmann 1964
33685.430	p	pg	-54165	0.00379	0.01745	Wachmann 1964
33709.385	s	pg	-54104.5	-0.02000	-0.00650	Wachmann 1964
34085.325	p	pg	-53156	-0.01189	-0.00097	Wachmann 1964
34087.305	p	pg	-53151	-0.01361	-0.00270	Wachmann 1964
34748.400	p	pg	-51483	-0.01971	-0.01313	Wachmann 1964
34769.400	p	pg	-51430	-0.02592	-0.01947	Wachmann 1964
34769.417	p	pg	-51430	-0.00842	-0.00197	Samus et al. 2004
34771.400	p	pg	-51425	-0.00764	-0.00120	Wachmann 1964
34773.375	p	pg	-51420	-0.01436	-0.00793	Wachmann 1964
34775.360	p	pg	-51415	-0.01108	-0.00466	Wachmann 1964
34776.345	s	pg	-51412.5	-0.01693	-0.01053	Wachmann 1964
34780.315	s	pg	-51402.5	-0.01037	-0.00399	Wachmann 1964
35129.495	s	pg	-50521.5	-0.00907	-0.00486	Wachmann 1964
35131.480	s	pg	-50516.5	-0.00579	-0.00159	Wachmann 1964
35160.415	s	pg	-50443.5	-0.00387	0.00014	Wachmann 1964
35161.405	p	pg	-50441	-0.00473	-0.00072	Wachmann 1964
35163.385	p	pg	-50436	-0.00645	-0.00245	Wachmann 1964
35164.390	s	pg	-50433.5	0.00769	0.01168	Wachmann 1964
35165.365	p	pg	-50431	-0.00816	-0.00418	Wachmann 1964
35184.390	p	pg	-50383	-0.00766	-0.00379	Wachmann 1964
35185.375	s	pg	-50380.5	-0.01352	-0.00965	Wachmann 1964

Table 6—Continued

Hel.JD	Type	Method	E	$(O - C)_1$	$(O - C)_2$	Reference
35186.370	p	pg	-50378	-0.00937	-0.00552	Wachmann 1964
35399.595	p	pg	-49840	-0.01722	-0.01465	Wachmann 1964
35459.460	p	pg	-49689	-0.00011	0.00210	Wachmann 1964
36214.475	p	pg	-47784	-0.01964	-0.02173	Wachmann 1964
36983.415	p	pg	-45844	0.01381	0.00766	Wachmann 1964
37693.455	s	pg	-44052.5	0.00427	-0.00528	Wachmann 1964
37694.440	p	pg	-44050	-0.00159	-0.01114	Wachmann 1964
37695.435	s	pg	-44047.5	0.00255	-0.00701	Wachmann 1964
45022.476	p	pg	-25561	0.03785	0.01044	IBVS No.2344
46004.632	p	vis	-23083	0.05444	0.02705	BBSAG No.74
46039.503	p	vis	-22995	0.04721	0.01983	BBSAG No.75
46350.643	p	vis	-22210	0.05749	0.03025	BBSAG No.78
46406.512	p	vis	-22069	0.04205	0.01483	BRNO No.27
46412.451	p	vis	-22054	0.03589	0.00868	BBSAG No.79
46744.594	p	vis	-21216	0.04297	0.01598	BBSAG No.82
46877.370	p	vis	-20881	0.04387	0.01698	BBSAG No.93
47068.604	s	vis	-20398.5	0.04209	0.01537	BBSAG No.85
47170.465	s	vis	-20141.5	0.04279	0.01617	BBSAG No.87
47531.335	p	vis	-19231	0.04195	0.01573	BBSAG No.90
47562.420	s	vis	-19152.5	0.01398	-0.01219	BBSAG No.91
47565.412	p	vis	-19145	0.03340	0.00723	BRNO No.30
47565.414	p	vis	-19145	0.03540	0.00923	BRNO No.30
47801.635	p	vis	-18549	0.03563	0.00976	BBSAG No.92
47838.701	s	vis	-18455.5	0.04350	0.01769	BBSAG No.93
47840.667	s	vis	-18450.5	0.02778	0.00197	BBSAG No.93
47842.661	s	vis	-18445.5	0.04006	0.01426	BBSAG No.93
47859.503	p	vis	-18403	0.03746	0.01168	BBSAG No.93
47880.505	p	vis	-18350	0.03325	0.00750	BBSAG No.93
47885.464	s	vis	-18337.5	0.03796	0.01221	BBSAG No.93
47946.298	p	vis	-18184	0.03322	0.00756	BAV No.56
47947.288	s	vis	-18181.5	0.03236	0.00670	BAV No.56
47947.295	s	vis	-18181.5	0.03936	0.01370	BBSAG No.94
47947.484	p	vis	-18181	0.03019	0.00453	BAV No.56
48153.587	p	vis	-17661	0.03452	0.00918	BBSAG No.96
48265.366	p	vis	-17379	0.04463	0.01947	BBSAG No.97
48934.593	s	vis	-15690.5	0.04548	0.02156	LBBSAG No.102
49009.492	s	vis	-15501.5	0.03555	0.01178	BBSAG No.103

Table 6—Continued

Hel.JD	Type	Method	E	$(O - C)_1$	$(O - C)_2$	Reference
50832.2573	s	ccd	-10902.5	0.01669	-0.00226	IBVS No.4888
50841.3736	s	ccd	-10879.5	0.01709	-0.00183	IBVS No.4888
50852.6602	p	ccd	-10851	0.00790	-0.01099	BBSAG No.117
50872.2967	s	vis	-10801.5	0.02539	0.00656	BRNO No.32
51129.5117	s	ccd	-10152.5	0.01341	-0.00458	BRNO No.32
51199.0712	p	pe	-9977	0.01461	-0.00314	Yang & Liu 2001
51199.2689	s	pe	-9976.5	0.01413	-0.00361	Yang & Liu 2001
51200.0618	s	pe	-9974.5	0.01435	-0.00340	Yang & Liu 2001
51200.2596	p	pe	-9974	0.01398	-0.00377	Yang & Liu 2001
51201.2507	s	pe	-9971.5	0.01422	-0.00352	Yang & Liu 2001
51455.8920	p	ccd	-9329	0.00476	-0.01209	Paschke Anton*
51841.5354	p	ccd	-8356	0.00585	-0.00959	IBVS No.5287
51876.6169	s	ccd	-8267.5	0.01095	-0.00437	IBVS No.5583
51952.5107	p	ccd	-8076	0.00495	-0.01007	BBSAG No.124
52209.5375	s	ccd	-7427.5	0.00293	-0.01108	BRNO No.34
52321.3059	s	ccd	-7145.5	0.00244	-0.01112	BRNO No.34
52338.3479	s	ccd	-7102.5	0.00167	-0.01183	BBSAG No.127
52602.9056	p	ccd	-6435	0.00002	-0.01237	IBVS No.5378
52689.3079	p	ccd	-6217	-0.00058	-0.01261	IBVS No.5438
52705.1581	p	ccd	-6177	-0.00412	-0.01608	Present paper
52944.3513	s	ccd	-5573.5	-0.00428	-0.01520	Present paper
52945.3402	p	ccd	-5571	-0.00623	-0.01715	Present paper
52973.8783	p	ccd	-5499	-0.00487	-0.01566	IBVS No.5493
52981.4090	p	pe	-5480	-0.00470	-0.01546	IBVS No.5676
53051.5611	p	pe	-5303	-0.00542	-0.01586	IBVS No.5603
53055.1282	p	ccd	-5294	-0.00541	-0.01584	IBVS No.5592
53082.2785	s	pe	-5225.5	-0.00464	-0.01495	IBVS No.5583
53375.5680	s	vis	-4485.5	-0.00940	-0.01835	OEJV No.03
53407.4759	p	ccd	-4405	-0.00716	-0.01596	IBVS No.5741
53409.4576	p	ccd	-4400	-0.00717	-0.01597	IBVS No.5741
53632.5958	p	ccd	-3837	-0.01041	-0.01815	BRNO No.34
53672.6266	p	ccd	-3736	-0.01031	-0.01785	IBVS No.5731
54154.3830	s	ccd	-2520.5	-0.00954	-0.01467	IBVS No.5802
54494.6405	p	pe	-1662	-0.01301	-0.01636	IBVS No.5870
54505.3422	p	ccd	-1635	-0.01259	-0.01588	IBVS No.5918
54512.6751	s	ccd	-1616.5	-0.01205	-0.01530	IBVS No.5875
54840.4509	s	ccd	-789.5	-0.01239	-0.01385	IBVS No.5918

Table 6—Continued

Hel.JD	Type	Method	E	$(O - C)_1$	$(O - C)_2$	Reference
54841.4409	p	pe	-787	-0.01325	-0.01471	IBVS No.5918
54874.7337	p	pe	-703	-0.01331	-0.01458	IBVS No.5894
54917.14338	p	ccd	-596	-0.01239	-0.01343	Present paper
55135.32692	s	ccd	-45.5	-0.01600	-0.01580	Present paper
55138.30024	p	ccd	-38	-0.01526	-0.01504	Present paper
55152.37052	p	ccd	-2.5	-0.01517	-0.01488	Present paper
55153.36144	s	ccd	0	-0.01511	-0.01481	Present paper

* The data from O-C gateway, <http://var.astro.cz/ocgate/ocgate.php?star=v396+mon&lang=en>

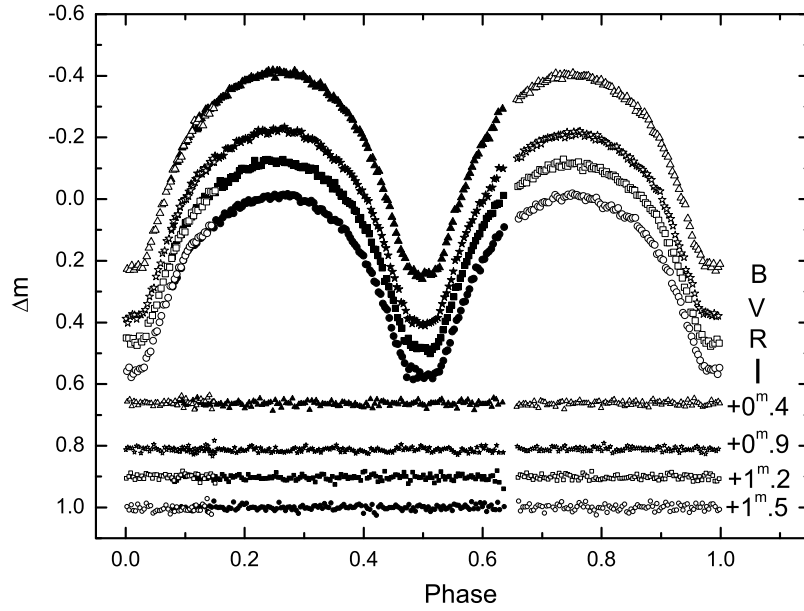


Fig. 1.— Observed multiple-color light curves in $BVRI$ bands for V396 Mon. Solid symbols are denote the data got in 2009-11-16; open symbols are denote the data got in 2009-11-17.

Table 7: Photometric solutions for V396 Mon.

Parameters	Photometric elements	errors
$g_1 = g_2$	0.32	assumed
$A_1 = A_2$	0.50	assumed
$x_{1bol} = x_{2bol}$	0.644	assumed
$y_{1bol} = y_{2bol}$	0.231	assumed
$x_{1B} = x_{2B}$	0.817	assumed
$y_{1B} = y_{2B}$	0.215	assumed
$x_{1V} = x_{2V}$	0.728	assumed
$y_{1V} = y_{2V}$	0.269	assumed
$x_{1R} = x_{2R}$	0.635	assumed
$y_{1R} = y_{2R}$	0.276	assumed
$x_{1I} = x_{2I}$	0.543	assumed
$y_{1I} = y_{2I}$	0.263	assumed
T_1	6210K	assumed
q	2.554	± 0.004
Ω_{in}	6.0187	–
Ω_{out}	5.4076	–
T_2	6121K	$\pm 3K$
i	89.°654	± 0.863
$L_1/(L_1 + L_2)(B)$	0.3194	± 0.0007
$L_1/(L_1 + L_2)(V)$	0.3146	± 0.0006
$L_1/(L_1 + L_2)(R)$	0.3119	± 0.0164
$L_1/(L_1 + L_2)(I)$	0.3099	± 0.0005
$\Omega_1 = \Omega_2$	5.9032	± 0.0074
$r_1(pole)$	0.2898	± 0.0007
$r_1(side)$	0.3034	± 0.0008
$r_1(back)$	0.3428	± 0.0015
$r_2(pole)$	0.4429	± 0.0006
$r_2(side)$	0.4750	± 0.0008
$r_2(back)$	0.5049	± 0.0010
f	18.9 %	$\pm 1.2 \%$
$\sum (O - C)_i^2$	0.000005618	

Table 8: A sample of shallow contact binaries with long-term period decrease.

Name	Period (d)	dP/dt (d/yr)	$i(^{\circ})$	$M_1(M_{\odot})$	$M_2(M_{\odot})$	q_{sp}	q_{ph}	$f(\%)$	Subtype	Spectrum
V417 Aql	0.3703	-5.5×10^{-8}	84.5	1.395	0.505	0.362	0.368	19	W	G2V
SS Ari	0.406	-4.03×10^{-7}	75.3	1.343	0.406	0.302	0.295	13	W	G0V
TY Boo	0.3171	-2.99×10^{-8}	76.6	0.93	0.4	0.437	0.466	10	W	G5V
RW Com	0.2373	-4.1×10^{-9}	75.2	0.92	0.31	0.337	0.343	17	W	K0V
CC Com	0.2211	-4.39×10^{-8}	90	0.69	0.36	0.522	0.518	20	W	K5V
BI CVn	0.3842	-1.51×10^{-7}	69.2	1.646	0.679	0.413	0.865	17	A	F2V
V1073 Cyg	0.7859	-9.20×10^{-6}	68.4	1.6	0.51	0.319	0.32	4	A	F2V
FT Lup	0.4701	-1.7×10^{-7}	84.7			0.43	0.45	12		F0+K2V
U Peg	0.3748	-2.1×10^{-8}	77.5	1.149	0.379	0.33	0.331	9	W	G2V
AU Ser	0.3865	-5.2×10^{-8}	80.6	0.921	0.646	0.701	0.7	9	A	K0V
AH Tau	0.3327	-6.98×10^{-8}					0.502	9		G1V
BM UMa	0.2712	-7.49×10^{-8}	89.5				0.54	17		K0V

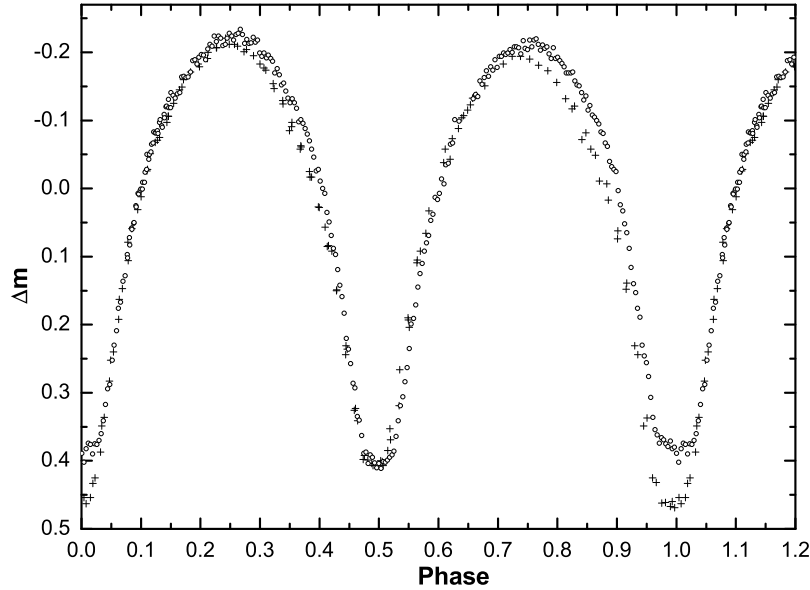


Fig. 2.— Comparison between the V light curves obtained by Yang & Liu (2001) in 1999 (crosses) and by us in 2009 (circles). The change of the light curve from phase 0.70P to 0.05P is clearly seen.

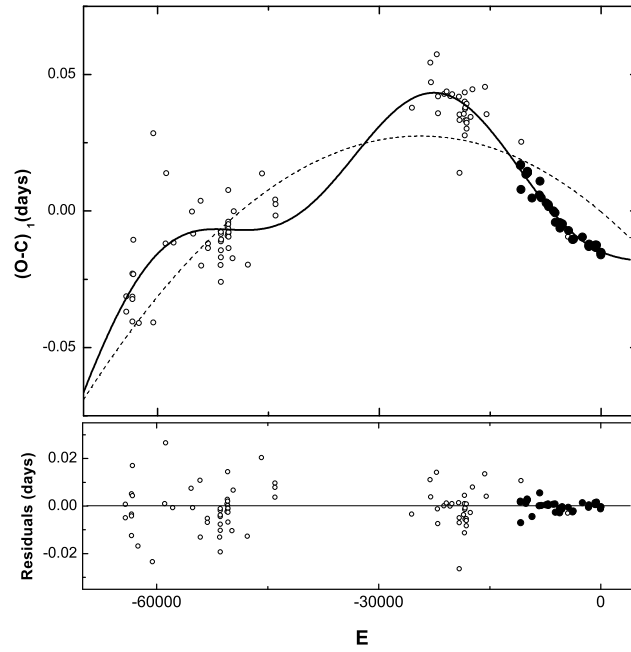


Fig. 3.— The $(O - C)$ diagram of V396 Mon formed by all available measurements. The $(O - C)_1$ values were computed by using a newly determined linear ephemeris (Eq.1). Solid circles refer to the pe and CCD data and open ones to the visual and pg data. The dashed line represents the quadratic fit; the solid line represents quadratic fit superimposed on a cyclic variation (Eq.3). The lower panel plots the residuals for Equation 3.

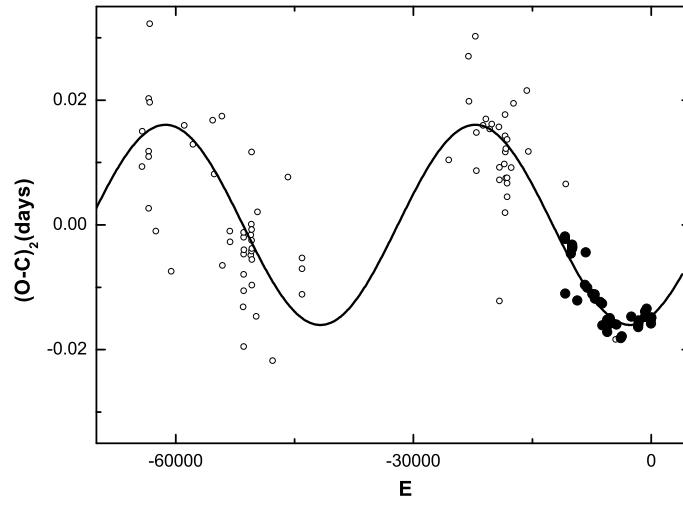


Fig. 4.— $(O - C)_2$ values for V396 Mon with respect to the quadratic ephemeris in Eq.(3). The symbols are the same as figure 3. The solid line represents the theoretical orbit of an assumed third body.

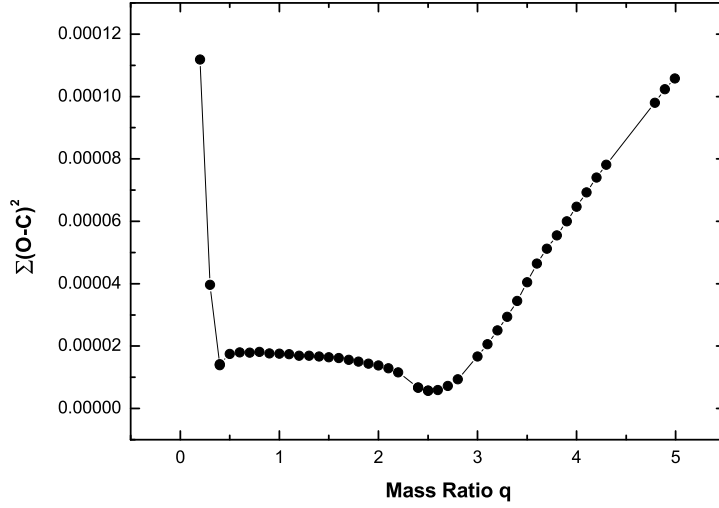


Fig. 5.— The relation between the mass ratio q and the sum of the squares of the residuals Σ for V396 Mon.

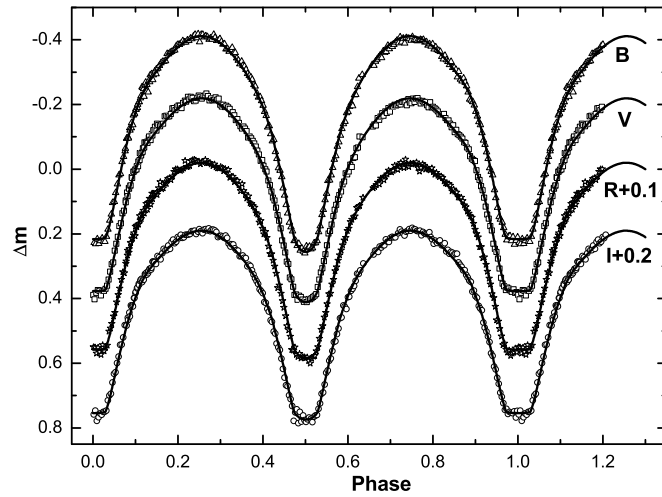


Fig. 6.— Observed (circles) and theoretical (solid curves) light curves in the $BVRI$ bands for V396 Mon.

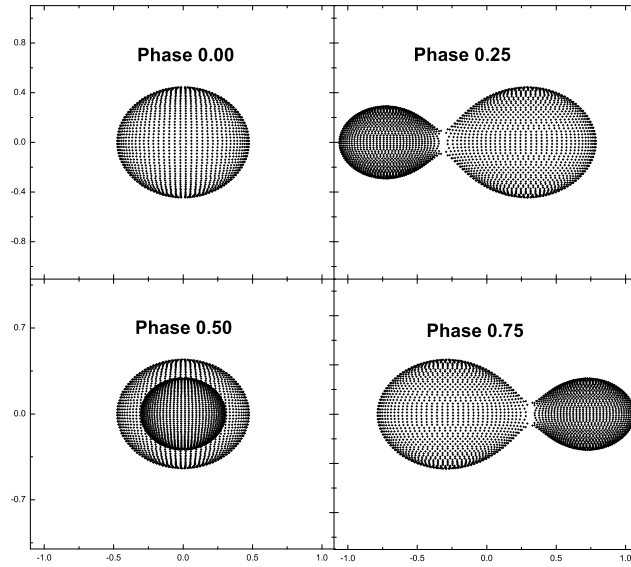


Fig. 7.— Geometrical structure of the shallow contact binary V396 Mon at phases 0.00P, 0.25P, 0.50P and 0.75P.